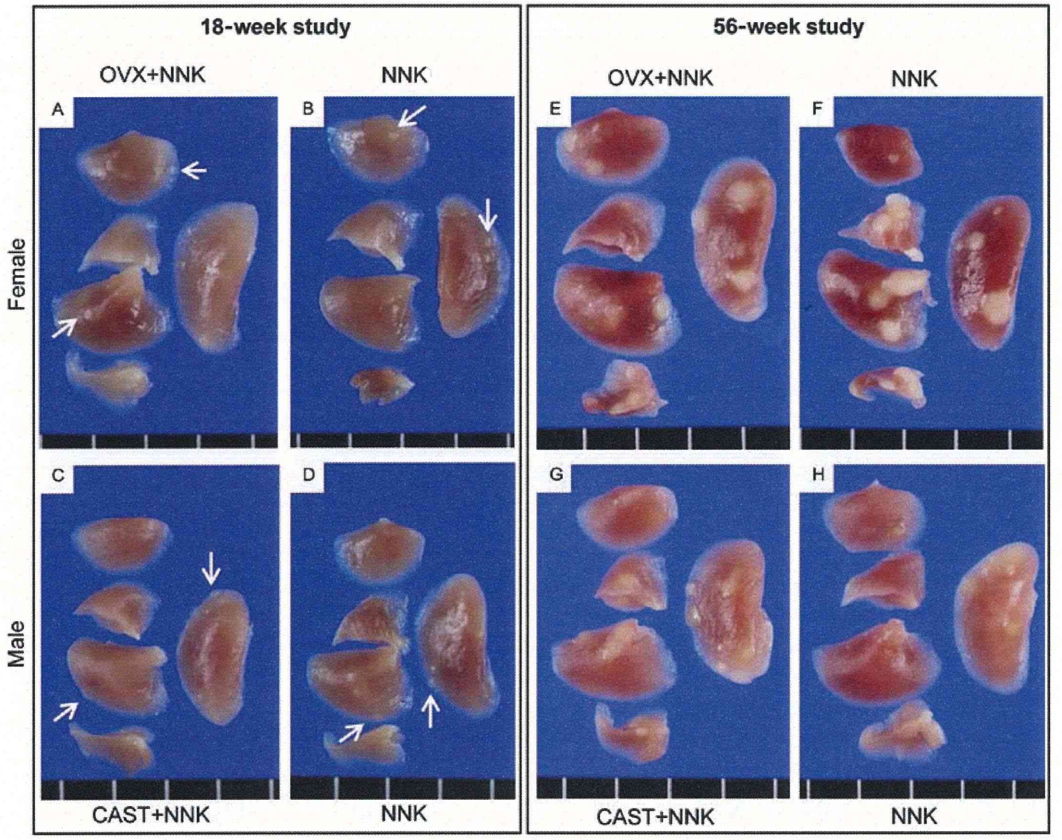


Figure 1. Macroscopical lung nodules. (A-D) In the 18-week study, small white nodules were observed in all groups (arrows indicate representative nodules in Groups 1-4). The sizes of the nodules observed in the 56-week study (E-H) were clearly larger than after 18 weeks (A-D). (A) Female ovariectomized group, Group 1; (B) female unoperated group, Group 2; (C) male castrated group, Group 3; (D) male unoperated group, Group 4; (E) female ovariectomized group, Group 5; (F) female unoperated group, Group 6; (G) male castrated group, Group 7; (H) male unoperated group, Group 8. OVX, ovariectomy; CAST, castration.

males of both 18- and 56-week studies. In the 56-week study, the multiplicity of lung nodules in the male castrated group (Group 7) was significantly increased as compared to the male unoperated group (Group 8).

*Histopathological analysis*. In histopathological analysis of lung proliferative lesions, bronchiolo-alveolar hyperplasias and adenomas were observed in the 18-week study (Groups 1-4) and bronchiolo-alveolar hyperplasias, adenomas and adenocarcinomas after 56 weeks (Groups 5-8) (Fig. 2). Incidences and multiplicities of each proliferative lesion are summarized in Table IV. The incidences showed no significant intergroup variation in either 18- or 56-week studies. In the 18-week study, the multiplicity of adenomas in the female ovariectomized group (Group 1) was significantly lower than in the female unoperated group (Group 2). In the 56-week study, the multiplicities of hyperplasias, adenomas and tumors (adenomas and adenocarcinomas) in the male castrated group (Group 7) were significantly increased, and carcinomas showed a tendency to increase, compared with the male unoperated group (Group 8). In liver, a hepatocellular carcinoma was observed in only one case of Group 5. No other lesions were observed in liver histopathologically. There were no lesions detected in kidneys in any of the groups. A lipoma surrounding the kidney and a thymoma were observed in Group 5, each at incidences of 1/18 (6%). No other tumors were observed in any of the groups.

## Discussion

In the present 18-week study, the serum concentration of estradiol of female mice was significantly decreased by ovariectomy, while the concentration of testosterone was slightly increased, and the serum concentration of testosterone of male mice was significantly decreased by castration. Estradiol is one of the most important sex steroid hormones secreted by the ovary and testosterone is a principal androgen secreted by the testis (23,24). The decrease with gonadectomy was in line with expectation and the increase in testosterone in ovariectomized females may be due to the secretion by the adrenal cortex. It is known that steroid sex hormones, particularly androgen, are also secreted from adrenal cortex (25), and secretion may be augmented in ovariectomized female mice as a reaction to ovariectomy (26). However, the concentration of testosterone in ovariectomized female mice was much lower than that in unoperated males.

In males, body weights showed no significant difference with castration after both 18 and 56 weeks. In females of the 56-week study, body weights in the operated group (Group 5) were significantly increased and this seemed to be due to the ovariectomy. In ovariectomized female mice, increase of body fat, reduction of lipid metabolism and activation of lipid synthesis have been reported (27-29). In males of the 18- and 56-week studies, the liver and kidney weights of

Table IV. Incidences and multiplicities of lung proliferative lesions.

| Group | Gender[a] | Treatment[a] | | Duration[b] | No.[c] | Hyperplasia | | Adenoma | | Adenocarcinoma | | Tumor[d] | |
|---|---|---|---|---|---|---|---|---|---|---|---|---|---|
| | | | | | | Incidence (%) | Multiplicity[e] | Incidence | Multiplicity | Incidence | Multiplicity | Incidence | Multiplicity |
| 1 | F | NNKx2 | OVX | 18 | 21 | 21/21 (100.0) | 4.8±3.6 | 18/21 (85.7) | 3.1±2.3[f] | 0/21 (0.0) | 0 | - | - |
| 2 | F | NNKx2 | N | 18 | 15 | 14/15 (93.3) | 3.7±2.4 | 15/15 (100.0) | 5.8±3.7 | 0/15 (0.0) | 0 | - | - |
| 3 | M | NNKx2 | CAST | 18 | 16 | 16/16 (100.0) | 5.3±2.9 | 14/16 (87.5) | 2.9±2.8 | 0/15 (0.0) | 0 | - | - |
| 4 | M | NNKx2 | N | 18 | 15 | 13/15 (86.7) | 4.1±2.7 | 14/15 (93.3) | 3.3±2.0 | 0/15 (0.0) | 0 | - | - |
| 5 | F | NNKx1 | OVX | 56 | 18 | 17/18 (94.4) | 5.3±3.5 | 18/18 (100.0) | 9.7±3.8 | 9/18 (50.0) | 0.9±1.0 | 18/18 (100.0) | 10.6±4.2 |
| 6 | F | NNKx1 | N | 56 | 12 | 11/12 (91.7) | 4.8±2.7 | 12/12 (100.0) | 10.2±4.6 | 7/12 (58.3) | 0.8±0.8 | 12/12 (100.0) | 11.0±4.5 |
| 7 | M | NNKx1 | CAST | 56 | 19 | 19/19 (100.0) | 4.5±2.2[g] | 19/19 (100.0) | 4.9±3.7[g] | 9/19 (47.4) | 0.7±1.1 | 19/19 (100.0) | 5.6±4.0[g] |
| 8 | M | NNKx1 | N | 56 | 14 | 14/14 (100.0) | 3.1±1.1 | 12/14 (85.7) | 2.5±1.7 | 4/14 (28.6) | 0.3±0.5 | 12/14 (85.7) | 2.8±2.0 |

[a]F, female; M, male; OVX, ovariectomy; CAST, castration; N, unoperated. [b]Weeks. [c]Number of mice examined. [d]Adenoma and adenocarcinoma. [e]Means ± standard deviation. [f]Significantly different from Group 2 by Welch's t-test ($P<0.05$). [g]Significantly different from Group 8 by Welch's t-test ($P<0.05$).




Figure 2. Histopathological lung proliferative lesions. Representative histopathology of lung lesions in the 56-week study. Bar, 50 $\mu$m. (A) Bronchiolo-alveolar hyperplasia in a Group-7 mouse; (B) adenoma in a Group-6 mouse; (C) adenocarcinoma in a Group-5 mouse.

castrated groups (Groups 3 and 7) were significantly decreased compared with the unoperated groups (Groups 4 and 8), and this may be due to the castration, as similar weight loss has been reported in castrated CF-1 mice (30). In females in the 18-week study, the liver weight of the ovariectomized group (Group 1) showed significant increase compared with the unoperated group (Group 2), although no such difference was noted after 56 weeks. As there is no report to support this, the liver weights may be influenced by estradiol derived from the ovary.

In unoperated groups, the multiplicities of lung nodules in females (Groups 2 and 6) were significantly greater than in males (Groups 4 and 8), confirming female A/J mice to be more susceptible to NNK-induced lung carcinogenesis

than males. Our results indicated that lung carcinogenesis was increased by castration, suggesting the possibility that testosterone inhibits NNK-induced lung carcinogenesis. In addition, the results of the 18-week study suggest that female sex hormones contribute to the malignant transformation of lung proliferative lesions, such as tumorous alteration from hyperplasia to adenoma. However, the results of the 56-week study did not support this suggestion.

In humans, there have been several reports that sex hormones affect incidences of lung adenocarcinoma. The characteristics of gene mutations in lung cancer are reported to differ between the sexes. In human lung cancer, tobacco-related p53 and EGFR mutations are more common in women than in men (20). Thus, there is a possibility that lung carcinogenesis progresses through different pathways between men and women. Estradiol influences the activity of various metabolic enzymes, such as CYP2A6, CYP1A2, CYP3A4, CYP2C19, UDP-glucuronyltransferase, which can activate NNK to ultimate carcinogenic species (2,31,32). In women, nicotine metabolism by CYP2A6 is reported to be accelerated by estrogen (33). Previously, we demonstrated that CYP2A6 plays important roles in NNK-induced lung carcinogenesis (5-9). In addition, oral contraceptives (estrogen) increase drug metabolism by glucuronidation (34-36). However, there are also reports that oral contraceptives decelerate drug metabolism by CYP1A2, CYP3A4 and CYP2C19 (37-39). Whatever the case, it appears clear that metabolic enzymes of NNK are influenced by estradiol. There is also the possibility that androgen influences lung carcinogenesis. Androgen receptors are present in human lung adenocarcinomas and normal lung tissue of humans and mice, and their expression in normal lung tissue of mice may be affected by castration and testosterone administration (40).

In male mice of the present study, tumors (adenomas and adenocarcinomas) were significantly increased in the castrated group only after 56 weeks, indicating that it is necessary to use long-term experiments in order to determine modifying potential of male sex hormones on lung carcinogenesis. The present study, in fact, pointed to the possibility that NNK-induced lung carcinogenesis may be inhibited by testosterone and accelerated by estradiol, although the effect was only slight in females. One explanation is that lung carcinogenic effects of NNK are so strong in females, that modifying effects of estradiol are masked.

In conclusion, female A/J mice were confirmed to be more susceptible to NNK-induced lung carcinogenesis than males. In males, lung carcinogenesis was increased by castration, whereas in females, malignant transformation of lung proliferative lesions tended to be inhibited by ovariectomy. These results suggested that NNK-induced lung carcinogenesis is inhibited by testosterone and accelerated by estradiol. These findings indicate the possibility that sex hormones play important roles in determining sex differences in lung carcinogenesis in A/J mice initiated by NNK. Additional experiments are ongoing to confirm the effects of the sex hormones themselves.

## Acknowledgements

We thank Dr Malcolm A. Moore for his help in the critical reading of this manuscript.

## References

1. Balbo S, Upadhyaya P, Villalta PW, Qian X and Kassie F: DNA adducts in aldehyde dehydrogenase-positive lung stem cells of A/J mice treated with the tobacco specific lung carcinogen 4-(methylnitrosamino)-1-(3-pyridyl)-1-butanone (NNK). Chem Res Toxicol: Mar 12, 2013 (Epub ahead of print).
2. Akopyan G and Bonavida B: Understanding tobacco smoke carcinogen NNK and lung tumorigenesis (Review). Int J Oncol 29: 745-752, 2006.
3. Chen RJ, Chang LW, Lin P and Wang YJ: Epigenetic effects and molecular mechanisms of tumorigenesis induced by cigarette smoke: an overview. J Oncol 2011: 654931, 2011.
4. Belinsky SA, Devereux TR, Foley JF, Maronpot RR and Anderson MW: Role of the alveolar type II cell in the development and progression of pulmonary tumors induced by 4-(methylnitrosamino)-1-(3-pyridyl)-1-butanone in the A/J mouse. Cancer Res 52: 3164-3173, 1992.
5. Imaida K, Yokohira M and Kuno T: Detection of carcinogenic and modifying potentials by test compounds using a mouse lung carcinogenesis bioassay (Review). J Toxicol Pathol 20: 117-123, 2007.
6. Takeuchi H, Saoo K, Matsuda Y, *et al*: 8-Methoxypsoralen, a potent human CYP2A6 inhibitor, inhibits lung adenocarcinoma development induced by 4-(methylnitrosamino)-1-(3-pyridyl)-1-butanone in female A/J mice. Mol Med Rep 2: 585-588, 2009.
7. Takeuchi H, Saoo K, Matsuda Y, *et al*: Dose dependent inhibitory effects of dietary 8-methoxypsoralen on NNK-induced lung tumorigenesis in female A/J mice. Cancer Lett 234: 232-238, 2006.
8. Takeuchi H, Saoo K, Yokohira M, *et al*: Pretreatment with 8-methoxypsoralen, a potent human CYP2A6 inhibitor, strongly inhibits lung tumorigenesis induced by 4-(methylnitrosamino)-1-(3-pyridyl)-1-butanone in female A/J mice. Cancer Res 63: 7581-7583, 2003.
9. Yokohira M, Takeuchi H, Saoo K, *et al*: Establishment of a bioassay model for lung cancer chemoprevention initiated with 4-(methylnitrosamino)-1-(3-pyridyl)-1-butanone (NNK) in female A/J mice. Exp Toxicol Pathol 60: 469-473, 2008.
10. Kuno T, Yokohira M, Matsuda Y, *et al*: Lack of modifying potential of 8-methoxypsoralen in the promotion or progression stages of lung carcinogenesis in A/J female mice. Oncol Rep 20: 767-772, 2008.
11. Matsuda Y, Saoo K, Hosokawa K, *et al*: Post-initiation chemopreventive effects of dietary bovine lactoferrin on 4-(methylnitrosamino)-1-(3-pyridyl)-1-butanone-induced lung tumorigenesis in female A/J mice. Cancer Lett 246: 41-46, 2007.
12. Yamakawa K, Kuno T, Hashimoto N, *et al*: Molecular analysis of carcinogen-induced rodent lung tumors: Involvement of microRNA expression and Kras or Egfr mutations. Mol Med Rep 3: 141-147, 2010.
13. Yokohira M, Hashimoto N, Yamakawa K, Saoo K, Kuno T and Imaida K: Lack of promoting effects from physical pulmonary collapse in a female A/J mouse lung tumor initiated with 4-(methylnitrosamino)-1-(3-pyridyl)-1-butanone (NNK) with remarkable mesothelial cell reactions in the thoracic cavity by the polymer. Exp Toxicol Pathol 63: 181-185, 2011.
14. Yokohira M, Hashimoto N, Yamakawa K, *et al*: Lack of modifying effects of intratracheal instillation of quartz or dextran sulfate sodium (DSS) in drinking water on lung tumor development initiated with 4-(Methylnitrosamino)-1-(3-pyridyl)-1-butanone (NNK) in female A/J mice. J Toxicol Pathol 22: 179-185, 2009.
15. Miyazaki M, Yamazaki H, Takeuchi H, *et al*: Mechanisms of chemopreventive effects of 8-methoxypsoralen against 4-(methylnitrosamino)-1-(3-pyridyl)-1-butanone-induced mouse lung adenomas. Carcinogenesis 26: 1947-1955, 2005.
16. Igarashi M, Watanabe M, Yoshida M, *et al*: Enhancement of lung carcinogenesis initiated with 4-(*N*-hydroxymethylnitrosamino)-1-(3-pyridyl)-1-butanone by *Ogg1* gene deficiency in female, but not male, mice. J Toxicol Sci 34: 163-174, 2009.
17. Morita T: A statistical study of lung cancer in the annual of pathological autopsy cases in Japan, from 1958 to 1997, with reference to time trends of lung cancer in the world. Jpn J Cancer Res 93: 15-23, 2002.
18. Sobue T, Ajiki W, Tsukuma H, Oshima A, Hanai A and Fujimoto I: Trends of lung cancer incidence by histologic type: a population-based study in Osaka, Japan. Jpn J Cancer Res 90: 6-15, 1999.
19. Zang EA and Wynder EL: Differences in lung cancer risk between men and women: examination of the evidence. J Natl Cancer Inst 88: 183-192, 1996.

20. Belani CP, Marts S, Schiller J and Socinski MA: Women and lung cancer: epidemiology, tumor biology, and emerging trends in clinical research. Lung Cancer 55: 15-23, 2007.
21. Nishio M, Ohyanagi F, Horiike A, *et al*: Gefitinib treatment affects androgen levels in non-small-cell lung cancer patients. Br J Cancer 92: 1877-1880, 2005.
22. Mohr U (ed): International Classification of Rodent Tumors: The Mouse. 1st edition. Springer-Verlag, Berlin, 2001.
23. de Kretser DM: The Testis. In: Reproduction in Mammals: Hormonal Control of Reproduction. Austin CR and Short RV (eds). Vol 3. 2nd edition. Cambridge University Press, Cambridge, pp76-90, 1984.
24. Baird DT: The Ovary. In: Reproduction in Mammals: Hormonal Control of Reproduction. Austin CR and Short RV (eds). Vol 3. 2nd edition. Cambridge University Press, Cambridge, pp91-114, 1984.
25. Pelletier G, Luu-The V, Li S and Labrie F: Localization of type 5 17β-hydroxysteroid dehydrogenase mRNA in mouse tissues as studied by in situ hybridization. Cell Tissue Res 320: 393-398, 2005.
26. Matsuura S and Suzuki K: Morphological changes in the submandibular glands and in the X zone of the adrenal gland following ovariectomy in mice. Cell Tissue Res 246: 549-556, 1986.
27. Kamei Y, Suzuki M, Miyazaki H, *et al*: Ovariectomy in mice decreases lipid metabolism-related gene expression in adipose tissue and skeletal muscle with increased body fat. J Nutr Sci Vitaminol 51: 110-117, 2005.
28. Wu J, Wang X, Chiba H, *et al*: Combined intervention of soy isoflavone and moderate exercise prevents body fat elevation and bone loss in ovariectomized mice. Metabolism 53: 942-948, 2004.
29. Yamaguchi M, Katoh S, Morimoto C, *et al*: The hormonal responses of lipoprotein lipase activity and lipolysis in adipose tissue differ depending on the stage of the estrous cycle in female rats. Int J Obes Relat Metab Disord 26: 610-617, 2002.
30. Duffel MW, Graham JM and Ziegler DM: Changes in dimethylaniline N-oxidase activity of mouse liver and kidney induced by steroid sex hormones. Mol Pharmacol 19: 134-139, 1981.
31. Kamataki T, Fujita KI, Nakayama K, Yamazaki Y, Miyamoto M and Ariyoshi N: Role of human cytochrome P450 (CYP) in the metabolic activation of nitrosamine derivatives: application of genetically engineered *Salmonella* expressing human CYP. Drug Metab Rev 34: 667-676, 2002.
32. Wiener D, Doerge DR, Fang JL, Upadhyaya P and Lazarus P: Characterization of *N*-glucuronidation of the lung carcinogen 4-(methylnitrosamino)-1-(3-pyridyl)-1-butanol (NNAL) in human liver: importance of UDP-glucuronosyltransferase 1A4. Drug Metab Dispos 32: 72-79, 2004.
33. Benowitz NL, Lessov-Schlaggar CN, Swan GE and Jacob P III: Female sex and oral contraceptive use accelerate nicotine metabolism. Clinl Pharmacol Ther 79: 480-488, 2006.
34. Miners JO, Grgurinovich N, Whitehead AG, Robson RA and Birkett DJ: Influence of gender and oral contraceptive steroids on the metabolism of salicytic acid and acetylsalicylic acid. Br J Clin Pharmacol 22: 135-142, 1986.
35. Mitchell MC, Hanew T, Meredith CG and Schenker S: Effects of oral contraceptive steroids on acetaminophen metabolism and elimination. Clin Pharmacol Ther 34: 48-53, 1983.
36. Stoehr GP, Kroboth PD, Juhl RP, Wender DB, Phillips JP and Smith RB: Effect of oral contraceptives on triazolam, temazepam, alprazolam, and lorazepam kinetics. Clin Pharmacol Ther 36: 683-690, 1984.
37. Balogh A, Klinger G, Henschel L, Börner A, Vollanth R and Kuhnz W: Influence of ethinylestradiol-containing combination oral contraceptives with gestodene or levonorgestrel on caffeine elimination. Eur J Clin Pharmacol 48: 161-166, 1995.
38. Laine K, Tybring G and Bertilsson L: No sex-related differences but significant inhibition by oral contraceptives of CYP2C19 activity as measured by the probe drugs mephenytoin and omeprazole in healthy Swedish white subjects. Clin Pharmacol Ther 68: 151-159, 2000.
39. Slayter KL, Ludwig EA, Lew KH, Middleton E Jr, Ferry JJ and Jusko WJ: Oral contraceptive effects on methylprednisolone pharmacokinetics and pharmacodynamics. Clin Pharmacol Ther 59: 312-321, 1996.
40. Mikkonen L, Pihlajamaa P, Sahu B, Zhang FP and Jänne OA: Androgen receptor and androgen-dependent gene expression in lung. Mol Cell Endocrinol 317: 14-24, 2010.

Experimental and Toxicologic Pathology 65 (2013) 925–932

Contents lists available at SciVerse ScienceDirect

Experimental and Toxicologic Pathology

journal homepage: www.elsevier.de/etp

# Strain differences in pleural mesothelial cell reactions induced by potassium octatitanate fibers (TISMO) infused directly into the thoracic cavity

Masanao Yokohira[a], Yuko Nakano[a], Keiko Yamakawa[a], Sosuke Kishi[a], Fumiko Ninomiya[a], Kousuke Saoo[a,b], Katsumi Imaida[a,*]

[a] *Onco-Pathology, Department of Pathology and Host-Defense, Kagawa University, Kagawa 761-0793, Japan*
[b] *Diagnostic Pathology, Kaisei General Hospital, Kagawa 762-0007, Japan*

ARTICLE INFO

*Article history:*
Received 16 October 2012
Accepted 4 January 2013

*Keywords:*
TISMO
Lung
Mesothelioma
Mouse
Strain difference
$TiO_2$

ABSTRACT

Although we have previously reported that the fiber-shaped TISMO, morphologically similar to asbestos, can induce a severe mesothelial reaction in A/J mice, it is important to clarify any strain differences. In the present study, female A/J, C3H/HeN, ICR and C57BL/6 mice were therefore employed as test strains. At the beginning of the experiment, all mice underwent a left thoracotomy and direct administration of 3 mg of TISMO particles suspended in 0.2 ml saline into the left thorax. The experiment was terminated after 21 weeks and all groups were sacrificed and the mesothelium and main organs were examined histopathologically. To contribute to mechanistic analysis, iron staining with Berlin blue and Turnbull's blue, and immunostaining for calretinin were also performed. The present experiment demonstrated only minor strain differences in the degree of pleural reaction to TISMO. However, there was clear variation in the iron and lymphocyte accumulation in the pleura and in the liver. This difference in response to TISMO fibers in vivo is important information when considering the development of mesothelioma as an animal model and the extrapolation to human risk from such animal studies.



## 1. Introduction

The development of approaches for therapy of malignant mesothelioma is an urgent priority, and an appropriate animal model is necessary for this purpose. There have been reports of peritoneal mesothelioma induction by chemicals or fibers in conventional rats (Crosby et al., 2000; Kamstrup et al., 2002; Kim et al., 2006; Krajnow and Lao, 2000) or pleural mesotheliomas in genetically modified animals, like the p53 knock out mouse (Jongsma et al., 2008). Since the pleural malignant mesothelioma is the most common form of mesothelioma in humans (Moore et al., 2008), a bioassay model featuring similar lesions in otherwise normal animals would be optimal. However, there is only small information for pleural mesothelioma in experimental wild-type animals using direct infusion of particles into the thoracic cavity.

In a previous study we demonstrated pronounced mesothelial cell reactions on the left lung surfaces and parietal pleura after polymer gel infusion directly into the left cavity of the thorax with thoracotomy to examine the influence of physical pulmonary collapse (Yokohira et al., 2011). In a subsequent experiment (Yokohira et al., 2010), thoracotomy was performed to allow infusion of 3 kinds of test particles directly into the thoracic cavity of A/J mice. Fiber-shaped particles of potassium octatitanate (TISMO) and granular-shaped micro and nano size order particles of titanium dioxide ($TiO_2$) were employed (1.5 mg in 0.2 ml saline/mouse) and the experiment was terminated after 21 weeks to assess pleural reactions. Only the fiber-shaped TISMO, morphologically similar to asbestos, induced a severe reaction, apparently involving iron accumulation derived from endogenous sources. The results indicate that risk of mesothelial cell reactions may not depend solely on particle size but also on shape.

Whether there might be strain differences in mesothelial cell reactions to fibers was the subject of the present study employing 4 mouse strains, i.e. A/J, C3H/HeN, ICR and C57BL/6. The A/J mouse is the most susceptible to lung carcinogenesis with reports of a 40% incidence and 0.58 tumors/mouse developing spontaneously by 52 weeks of age (Shimkin and Stoner, 1975; Takeuchi et al., 2009). C57BL/6 mice appear to be inflammation-susceptible, while C3H animals are more inflammation-resistant (Backus-Hazzard et al., 2004; Gong, 2006; Page et al., 2007). C3H/HeN mice have been applied in an animal model to investigate the susceptibility of acute and chronic inflammation, infection and carcinogenesis (Alm et al., 2010) while ICR mice are recognized as having advantages for general multipurpose safety and efficacy testing (Charles

* Corresponding author at: Onco-Pathology, Department of Pathology and Host-Defense, Faculty of Medicine, Kagawa University, 1750-1, Ikenobe, Miki-cho, Kita-gun, Kagawa 761-0793, Japan. Tel.: +81 87 891 2111; fax: +81 87 891 2112.
*E-mail address:* imaida@med.kagawa-u.ac.jp (K. Imaida).

0940-2993/$ – see front matter © 2013 Elsevier GmbH. All rights reserved.
http://dx.doi.org/10.1016/j.etp.2013.01.006

**Table 1**
Body weights and relative organ weights.

| Groups<br>Strain | 1<br>A/J | 2<br>ICR | 3<br>C3H/HeN | 4<br>C57BL/6 |
|---|---|---|---|---|
| No. | 15 | 16 | 12 | 14 |
| Body weight (g) | 24.3 ± 3.4[b,c] | 47.1 ± 8.2[a,c,d] | 32.5 ± 4.9[a,b,d] | 26.6 ± 3.45[b,c] |
| Lung | | | | |
| Absolute (g) | 0.22 ± 0.03[b,c,d] | 0.37 ± 0.07[a,c,d] | 0.29 ± 0.05[a,b] | 0.29 ± 0.06[a,b] |
| Relative (%) | 0.93 ± 0.14 | 0.80 ± 0.19[c] | 0.91 ± 0.19[b] | 1.08 ± 0.19 |
| Liver | | | | |
| Absolute | 1.07 ± 0.16[b] | 1.85 ± 0.26[a,c,d] | 1.15 ± 0.12[b,d] | 1.06 ± 0.11[b,c] |
| Relative | 4.42 ± 0.39[b,c,d] | 3.99 ± 0.52[a,c] | 3.57 ± 0.26[a,b,d] | 4.00 ± 0.29[a,c] |
| Kidneys | | | | |
| Right | | | | |
| Absolute | 0.13 ± 0.01[b,c] | 0.18 ± 0.02[a,c,d] | 0.15 ± 0.02[a,b,d] | 0.12 ± 0.01[b,c] |
| Relative | 0.53 ± 0.06[b,d] | 0.41 ± 0.09[a] | 0.47 ± 0.05 | 0.45 ± 0.05[a] |
| Left | | | | |
| Absolute | 0.12 ± 0.02[b,d] | 0.18 ± 0.02[a,c,d] | 0.14 ± 0.02[b,d] | 0.11 ± 0.02[a,b,c] |
| Relative | 0.50 ± 0.04[b,c,d] | 0.40 ± 0.08[a] | 0.43 ± 0.06[a] | 0.40 ± 0.03[a] |

[a] $P<0.05$ vs. Group 1.
[b] $P<0.05$ vs. Group 2.
[c] $P<0.05$ vs. Group 3.
[d] $P<0.05$ vs. Group 4.

River Laboratories International 2012). To contribute to mechanistic analysis, iron staining with Berlin blue and Turnbull's blue for detecting $Fe^{3+}$ and $Fe^{2+}$, respectively, and immunostaining for calretinin were also performed.

## 2. Materials and methods

### 2.1. Chemicals

Potassium octatitanate fibers, trade name TISMO and chemical formula $K_2O{\cdot}nTiO_2$, were supplied by Otsuka Chemical Co., Ltd. (Osaka, Japan) with dimensions mostly shorter than 50 μm in length and less than 2 μm in width. Previously, we reported the scanning electron microscope (SEM) images of the TISMO fibers (Yokohira et al., 2010). The fiber particles were suspended in saline (Otsuka isotonic sodium chloride solution, Otsuka Pharmaceutical Factory, Inc., Tokushima, Japan).

### 2.2. Animals

Female A/J, C3H/HeN, ICR and C57BL/6 mice (5 weeks of age) were purchased and maintained in the Division of Animal Experiments, Life Science Research Center, Kagawa University, according to the Institutional Regulations for Animal Experiments. A/J mice (A/J Jms Slc) and C3H/HeN mice (C3H He N Slc) were from Japan SLC, Inc. (Shizuoka, Japan) and ICR mice (Crlj: CD1) and C57BL/6 mice (C57BL/6N CrlCrlj) were from Japan Charles River (Kanagawa, Japan). The regulations included the best considerations on animal welfare and good practice of animal handling contributing to the replacement, refinement and reduction of animal testing (3Rs). The protocol of the experiment was approved by the Animal Care and use Committee for Kagawa University. The animals were housed in polycarbonate cages with re-used paper chips (EchoChip®, CL-4163, CLEA Japan, Inc., Tokyo, Japan) for bedding and given free access to drinking water and a basal diet, Oriental MF (Oriental Yeast Co., Ltd., Tokyo, Japan), under controlled conditions of humidity (60 ± 10%), lighting (12-h light/dark cycle) and temperature (24 ± 2 °C). The experiments were started after a 2-week acclimation period.

### 2.3. Experimental design and tissue preparation

A total of 64 mice at 7 weeks of age were divided into 4 groups of 16 mice each, A/J mice (Group 1), ICR mice (Groups 2), C3H/HeN mice (Group 3) and C57BL/6 mice (Group 4). At the beginning of the experiment, all mice of Groups 1–4 underwent a left thoracotomy and administration of 3 mg of TISMO particles suspended in 0.2 ml saline. Each mouse was given an intraperitoneal injection of 0.2 ml pentobarbital sodium (Somunopentyl, Kyoritsu Seiyaku Co., Tokyo, Japan) with 10 times dilution (0.06–0.1 ml/10 g body weight). Under deep anesthesia, a skin incision (about 7 mm) was performed on the left axilla. After confirmation of the location of the thoracic wall, thoracotomy was completed with an incision (approximately 5 mm) between ribs. The left lung was observed directly through the opened hole and atelectasis was confirmed. After infusion of TISMO solution into the left thoracic cavity, the skin was clipped together to close the thorax. The experiment was terminated after 21 weeks and all groups were sacrificed under deep anesthesia (Yokohira et al., 2010).

At necropsy, the lungs, liver and kidneys were removed. The lungs were weighed including the trachea and heart first, then rinsed and infused with 10% neutral buffered formalin. The weights of lungs were finally calculated by subtraction of the weights of the trachea and heart. The organs were immersed in 10% neutral buffered formalin for a week and 2 slices of the left lobe of the lung and 1 slice each of the other lobes were routinely processed for embedding in paraffin and histopathological examination of H & E stained sections. The maximum visceral pleural thickness of the left lung was measured. From the measured data, the relative value was calculated, thickness (mm)/lung weight (g), to correct for strain differences in lung size. Sections were also prepared for special Berlin blue and Turnbull's blue staining to detect iron accumulation, for $Fe^{3+}$ and $Fe^{2+}$, respectively, in the lung, liver and kidney. In addition, immunostaining of calretinin was performed to identify mesothelial cells in the lung (Shield and Koivurinne, 2008).

### 2.4. Immunostaining analysis

The lungs were immunostained by the avidin–biotin complex (ABC) method, all processes from deparaffinization to counterstaining with hematoxylin being performed automatically using

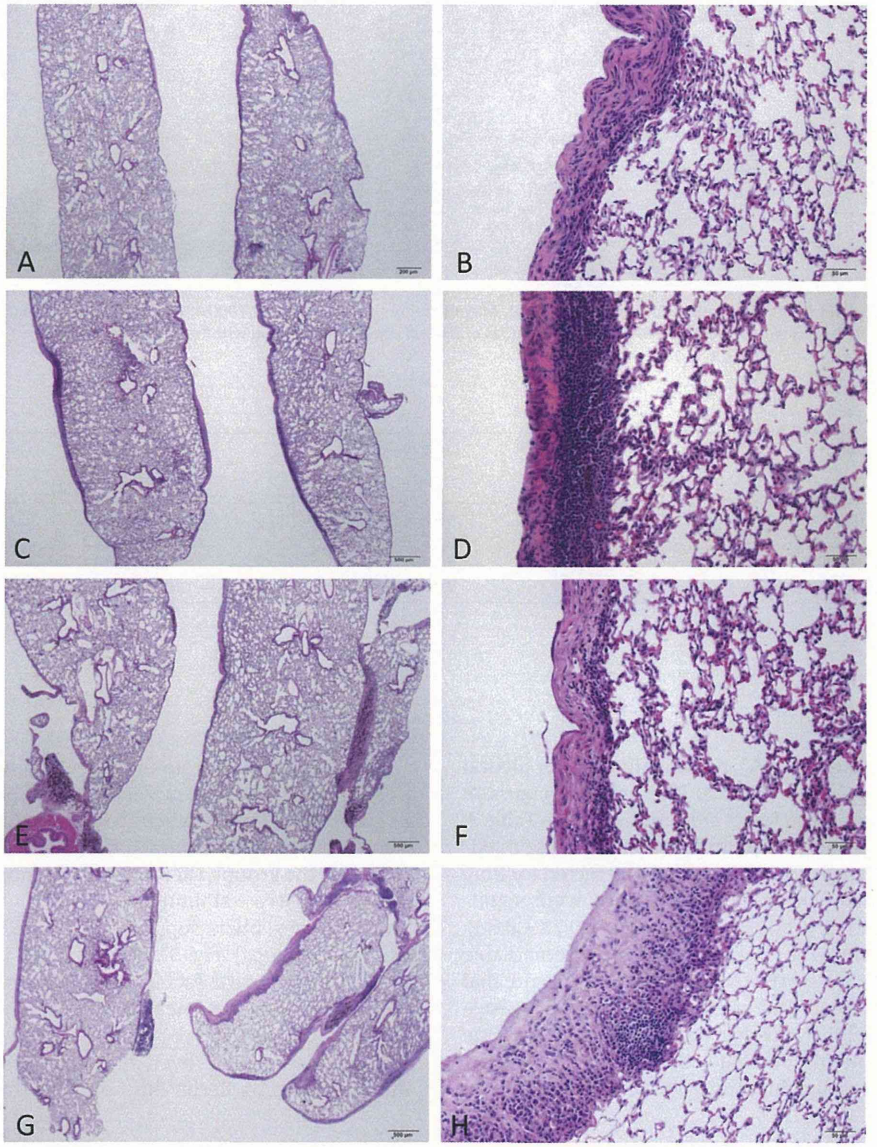


**Fig. 1.** Histopathological findings for lungs at week 21. (A and B) A/J mice (Group 1); (C and D) ICR mice (Group 2); (E and F) C3H/HeN mice (Group 3); (G and H) C57BL/6 mice (Group 4). Magnifications are 20× (A), 12.5× (C, E and G) and 100× (B, D, F and H). Thickened pleura with several fibers were observed in all groups. Inflammatory reactions were consistently limited to the pleura.

the Ventana Discovery™ staining system (Ventana Medical Systems, AZ, USA). Anti mouse calretinin monoclonal antibody, clone 5A5, purchased from Novocastra Laboratories Ltd. (Newcastle upon Tyne, UK) was employed at 1:100 dilution.

### 2.5. Statistical analysis

The data for body and organ weights and pleural thickness were analyzed by the Tukey–Kramer test (multi-comparison test).

## 3. Results

A total of 5 mice died (3 of Group 3 and 2 of Group 4) just after the thoracotomy due to the surgery or anesthesia. In addition, 2 mice (1 of Group 3 at week 17 and 1 of Group 1 at week 19) died before sacrifice. These deaths were considered accidental. General condition in all groups demonstrated no remarkable change during the experimental period. Final body and organ weights are shown in Table 1. The body weights of ICR mice (Group 2) (47.1 ± 8.2 g) were significantly greater than in the other groups, while those of A/J mice (Group 1) (24.3 ± 3.4 g) were the smallest. The relative weights for the lungs of C57BL/6 mice (Group 4) (1.08 ± 0.19%) were significantly greater than for ICR mice (Group 2) (0.80 ± 0.19%). The liver and kidney weights of A/J mice (Group 1) were significant greater than in the other groups.

Grossly, the infused TISMO fibers formed discrete masses in the cavity of the chest and severe adhesions around the lung, with a focus on the left lobe, to the thorax in all groups to almost the same degree.

Histopathologically, one A/J mouse (Group 1) showed glandular hyperplasia around the trachea in the lung and one A/J mouse had one adenoma. Pleural thickening with several fibers was observed in all groups (Fig. 1). Several masses formed by the TISMO fibers were observed in the pleura of the lung and some fibers existed isolated in the lung. Inflammatory reactions were limited to the pleura in all groups. One other A/J mouse featured granulation with

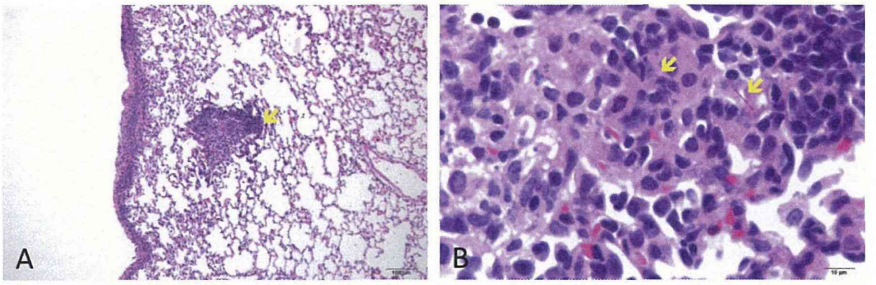


**Fig. 2.** Histopathological findings for lungs of A/J mice (Group 1) at week 21. Magnifications are 40× (A) and 1000× (B). One A/J mouse featured granulation (arrow) with some fibers in the lung field (A). Fibers (arrows) were detected not only in areas of pleural thickening but also within alveoli (B).

**Table 2**
Visceral pleural thickness.

| Groups | Strain | No. | Lung weight (g) | Maximum pleural thickness | |
|---|---|---|---|---|---|
| | | | | Thickness (mm) | Relative value[a] |
| 1 | A/J | 15 | 0.22 ± 0.03[c,d,e] | 0.32 ± 0.11 | 1.49 ± 0.66[c] |
| 2 | ICR | 16 | 0.37 ± 0.07[b,d,e] | 0.29 ± 0.12 | 0.78 ± 0.20[b] |
| 3 | C3H/HeN | 12 | 0.29 ± 0.05[b,c] | 0.31 ± 0.07 | 1.13 ± 0.27 |
| 4 | C57BL/6 | 14 | 0.29 ± 0.06[b,c] | 0.29 ± 0.15 | 1.05 ± 0.78 |

[a] Relative value = thickness (mm)/lung weight (g).
[b] $P < 0.05$ vs. Group 1.
[c] $P < 0.05$ vs. Group 2.
[d] $P < 0.05$ vs. Group 3.
[e] $P < 0.05$ vs. Group 4.

some fibers in the lung field (Fig. 2A), not only in areas of pleural thickening but also within alveoli (Fig. 2B). The average maximum visceral pleural thicknesses of left lungs are summarized in Table 2. There was no significant inter-group difference in absolute maximum pleural thickness. From the relative values corrected for lung weight, pleura of A/J mice (Groups 1) (1.49 ± 0.66) were significantly thicker compared with ICR mice (Group 2) (0.78 ± 0.50). Lymphoid cell infiltration into the thickened pleura was remarkable in ICR mice (Group 2) (Fig. 1D). In the thickened pleura, mesothelial cell infiltration was observed and confirmed by immunohistochemistry for calretinin (Fig. 3), the degree being almost the same in all groups. Though some mesothelial cells showed mild atypia, there was no evidence of malignancy, invasion or metastasis.

Positive Berlin blue staining ($Fe^{3+}$ staining) was detected in the areas of thickened pleura with TISMO fibers, but not in alveoli in all groups (Fig. 4). ICR mice (Group 2) showed the strongest iron accumulation to the pleura and C57BL/6 mice (Group 4) the least. In none of the groups, there were any lesions positive for Turnbull's blue staining ($Fe^{2+}$ staining).

In the liver, fibers supposed to be TISMO were detected in all rats (in all groups) (Fig. 5). A/J, ICR and C57BL/6 mice (Groups 1, 2 and 4) showed some foci with lymphocyte infiltration containing a few fibers around or near the portal veins (Fig. 5A–D, G and H). However, C3H/HeN mice (Group 3) showed much less of lymphocyte infiltration in the liver, although fibers were detected (Fig. 5E and F). Regarding Berlin blue staining (for $Fe^{3+}$), positive lesions

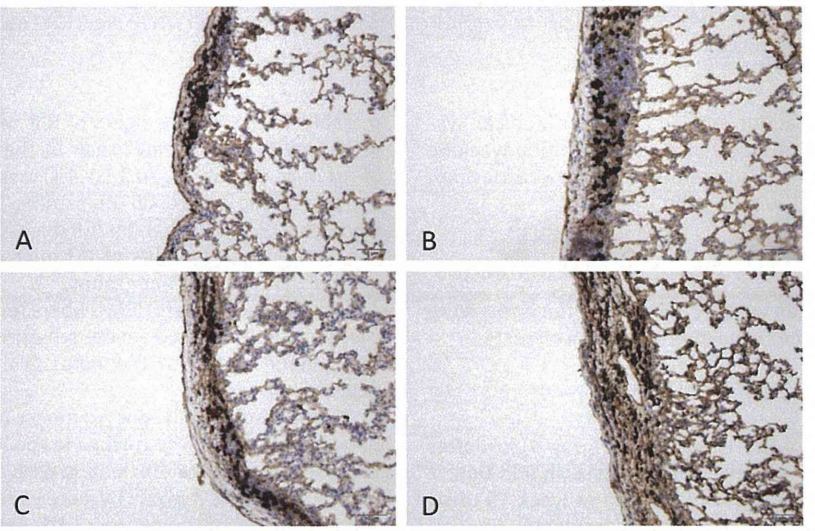


**Fig. 3.** Immunohistochemistry of calretinin. (A) A/J mice (Group 1); (B) ICR mice (Group 2); C, C3H/HeN mice (Group 3); (D) C57BL/6 mice (Group 4). The magnification is 100× (A–D). In the thickened pleura, mesothelial cell infiltration was observed to almost the same degree in all groups.

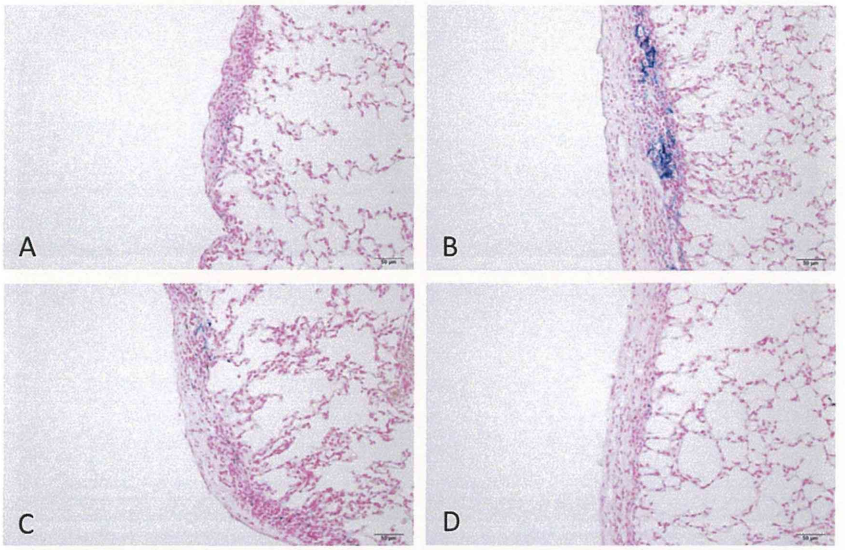


**Fig. 4.** Berlin blue staining ($Fe^{3+}$ staining) of the lungs. (A) A/J mice (Group 1); (B) ICR mice (Group 2); (C) C3H/HeN mice (Group 3); (D) C57BL/6 mice (Group 4). The magnification is 100× (A–D). Positive spots were detected in the areas of thickened pleura with TISMO fibers, but not in alveoli in all groups. ICR mice (Group 2) showed the strongest iron accumulation in the pleura (Fig. 3B) and C57BL/6 mice (Group 4) the least (Fig. 3D).

were observed around fibers rather than in foci of lymphocyte infiltration themselves (Fig. 6). Especially in C3H/HeN mice (Group 3), strong positive lesions with fibers also being seen with limited lymphocyte infiltration into the liver (Fig. 6C). Positive lesions of ICR and C3H/HeN mice (Group 2 and 3) were strong with almost same degree and A/J and C57BL/6 mice (Group 1 and 4) showed weak. In none of the groups, there were any lesions positive for TurnBull's blue staining (for $Fe^{2+}$), as in the lung. In the kidneys, no remarkable changes were detected by H & E nor Turnbull's blue staining. From Berlin blue staining, C3H/HeN and C57BL/6 mice (Group 3 and 4) showed clear positive lesions in proximal renal tubules but no fibers were detected in the kidneys (figure is not shown). Kidneys of A/J and ICR mice (Group 1 and 2) showed only slight positive lesions. Histopathological findings for thickness, existence of fibers, lymphocytes or $Fe^{3+}$ in the lung, liver and kidneys are summarized in Table 3.

## 4. Discussion

In the present experiment, there were clear mouse strain differences in the absolute body weights and relative weights of the lungs, livers and kidneys. However, there was no histopathological evidence, like inflammatory change, which could have contributed to the variation in relative organ weights.

Fibrous particles greater than 1 μm in length with a length-to-width ratio greater than 10:1 were early concluded to have particular biological relevance for mesothelial risk (Friedrichs and Molik, 1985). The TISMO used in our experiments, with dimensions mostly shorter than 50 μm in length and less than 2 μm in width, meets these criteria. In our previous experiments with TISMO fibers, administered by intratracheal instillation to F344 rats at 4 mg per rat, only mild inflammatory reactions were observed whereas severe inflammatory changes were induced by quartz particles in the lungs after 28 days (Yokohira et al., 2007, 2009). Other reports of TISMO administration by chronic inhalation also featured only limited inflammation in the lung (Ikegami et al., 2000, 2004). In the present experiment, one A/J mouse featured granulation with some fibers in the lung alveoli even though infusion was outside of the lung into the thoracic cavity. Thus fibers can pass through the pleura readily. We conclude that TISMO fibers in the lung alveoli induce mild inflammatory reactions in the acute phase and granulomatous change with persistent inflammation in the chronic phase.

Histopathologically, pleural thickening featuring fibers was observed in all groups with no significant strain differences. However, relative to body weights, pleura of ICR mice (Group 2) were significantly thinner as compared with those in A/J mice (Groups 1). Lung weights are a little low for reliability to use as a relative value because of exfoliation and severe adhesion to the thorax. Lung size, for example, the maximum length of the left lobe or the volume, is also not useful for due to low expansibility with severe adhesion. Though it is arguable that the relative value from lung weight reflects exact degree of pleural thickness or not, at least it is suitable as a reference.

The mesothelial cells in the thickened pleura showed only slight atypia and it proved difficult to give a diagnosis of malignancy. The

**Table 3**
Summary of histopathological findings.

| Groups | Strain | Lung | | | Liver | | | Kidneys | | |
|---|---|---|---|---|---|---|---|---|---|---|
| | | Pleural thickness (absolute/relative value) | Lymphocyte infiltration in the pleura | $Fe^{3+}$ in the pleura (Berlin blue) | Fibers | Lymphocyte infiltration foci | $Fe^{3+}$ around the fibers (Berlin blue) | Fibers | Lymphocyte infiltration | $Fe^{3+}$ in proximal tubules (Berlin blue) |
| 1 | A/J | ++/+++ | – | + | ++ | + | + | – | – | + |
| 2 | ICR | ++/+ | ++ | +++ | ++ | + | +++ | – | – | + |
| 3 | C3H/HeN | ++/++ | – | + | ++ | – | +++ | – | – | ++ |
| 4 | C57BL/6 | ++/++ | – | + | ++ | + | + | – | – | ++ |

+++, strong; ++, medium; +, weak; –, none to weak.

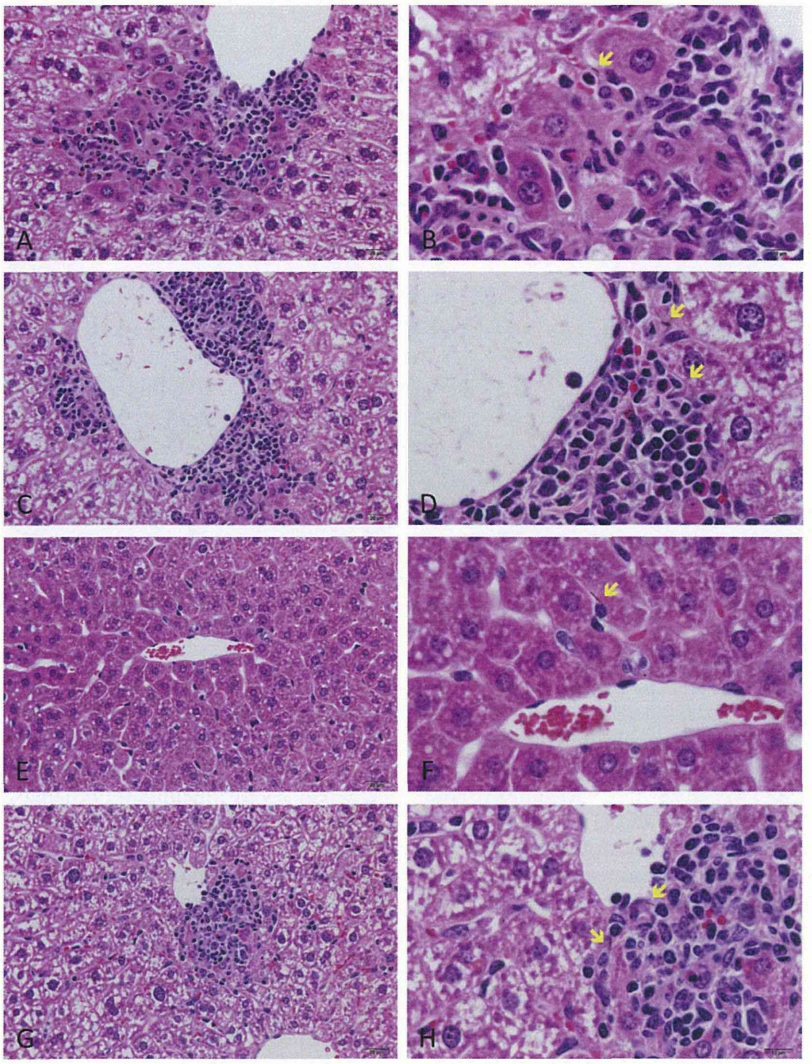


**Fig. 5.** Histopathological findings for livers at week 21. (A and B) A/J mice (Group 1); C and D, ICR mice (Group 2); E and F, C3H/HeN mice (Group 3); G and H, C57BL/6 mice (Group 4). Magnification is 400× (A, C, E and G) and 1000× (B, D, F and H). Arrows indicate fibers, considered to be TISMO fibers, these being detected in all groups. A/J, ICR and C57BL/6 mice (Groups 1, 2 and 4) showed some lesions of focal lymphocyte infiltration possessing some few fibers around or near the portal veins in the liver (A–D, G and H). C3H/HeN mice (Group 3) showed the less of lymphocyte infiltration in the liver, though the several fibers were detected (E and F).

experimental period of 21 weeks was decided based on an earlier report of mortality rate due to mesothelioma increase from about 130 days after intraperitoneal injection of MWCNT or crocidolite in p53-heterozygous mice (Takagi et al., 2008). However, for wild-type animals, 21 weeks appears to be too short for induction of malignant lesions. Now an experiment with a longer period is on-going in our laboratory in order to confirm malignant mesothelioma formation.

From the Berlin blue staining in the present experiment, iron accumulation ($Fe^{3+}$) was observed around the TSMO fibers in thickened pleura of the lung, almost co-locating with immunostaining for calretinin, indicative of mesothelioma cells. Interestingly, ICR mice (Group 2) showed the strongest iron accumulation in the pleura and C57BL/6 mice (Group 4) the least. The chemical formula of TISMO is $K_2O{\cdot}nTiO_2$ with no ferrous component. Iron as a component of asbestos or as a consequence of asbestos-induced pathology is a major candidate for underlying carcinogenic mechanisms because overload is recognized to be carcinogenic (Toyokuni, 1996). Iron works as a catalyst for the Fenton reaction ($Fe^{2+} + H_2O_2 > Fe^{3+} + OH^{\bullet} + OH^-$), thus promoting the generation of the undesirable molecule, hydroxyl radical ($OH^{\bullet}$) (Toyokuni, 2011). DNA damage and apoptosis because of iron-derived reactive oxygen species (ROS) are regarded as important for malignant mesothelioma development (Aung et al., 2007; Jiang et al., 2008; Kamp, 2009; Toyokuni et al., 1997). Respiratory exposure to asbestos is associated with mesothelioma in humans and electron spin resonance analyses has showed that crocidolite and amosite containing high amounts of iron, but not chrysotile, catalyze hydroxyl radical formation (Toyokuni, 2009). Erionite, a natural fibrous mineral zeolite, is known to be the most carcinogenic fiber, more than asbestos (Kleymenova et al., 1999; Wagner et al., 1985). Zeolite contains little to no iron or iron-exchangeable irons (Ruda and Dutta, 2005). Furthermore, intraperitoneal or intrascrotal application of multi-wall carbon nanotube (MWCNT) without any ferrous component has been also reported to induce mesotheliomas (Sakamoto et al., 2009; Takagi et al., 2008). From the report of the 4-week inhalation study on rats with two poorly soluble iron containing solid aerosols of siderite ($FeCO_3$) and magnetite ($Fe_3O_4$), despite its lower iron content, the exposure to $FeCO_3$ caused a more pronounced and sustained inflammation as compared to $Fe_3O_4$ (Pauluhn and Wiemann, 2011). There is also reported the effects of two different mineral dusts, iron oxide with high iron content and calcium tungstate with